Journal of
NANOSTRUCTURES
JNS
NANOSTRUCTURES
JNS.kashanu.ac.ir

Synthesis, Characterization and Photocatalytic Properties of $MnTiO_3$-Zeolite-Y Nanocomposites

M. Enhessari[a,*], M. Kargar-Razi[b], P. Moarefi[b], A. Parviz[c]

[a]*Department of Chemistry, Naragh Branch, Islamic Azad University, Naragh, P. O. Box. . 37961–58719 , Iran*
[b]*Department of Chemistry, North Tehran Branch, Islamic Azad University, Tehran, P. O. Box. 19136, Iran*
[c]*Department of Textile engineering, South Tehran Branch, Islamic Azad University, Tehran ,P. O. Box. 11365–4435, Iran*

Article history:
Received 2/10/2011
Accepted 26/1/2012
Published online 1/2/2012

Keywords:
$MnTiO_3$-Zeolite-Y nanocomposite
Sol-Gel method
Photocatalytic
Magnetic properties

**Corresponding author:*
E-mail address:
enhessari@ iau-naragh.ac.ir
Phone: +98 866 4463920
Fax: +98 866 4463920

Abstract

$MnTiO_3$-Zeolite-Y nanocomposites were synthesized with 5-10-20% (w/w) of $MnTiO_3$ by stearic acid gel method. Then, the gels were calcined at 900 °C for 4 hours and the resulted spectra were investigated at 20% (w/w) concentration. Also, the presence of rhombohedral phase of $MnTiO_3$ in Zeolite-Y matrix was confirmed by XRD, SEM, EDX and BET. The VSM results showed the antiferromagnetic properties for the 20% nanocomposite. The photocatalytic activity of the nanocomposites was finally evaluated by degradation of methylene blue and calcon reagents in aqueous solution.

1. Introduction

Undoubtedly, the textile industry produces dye pollutants as a major source of environmental contamination. It is estimated that 10 to 15 percent of dyestuff without treatment can be released in water during dyeing processes [1]. A variety of physical, chemical, and biological methods, such as adsorption, coagulation, membrane process, and oxidation-ozonation are presently available for treatment of dye wastewater [2–4]. The conventional processes are to a large extent insufficient to purify the wastewaters. They are just transferred from aqueous to another phase, thus causing secondary pollution problem [5, 6]. Nowadays, photo catalysis technique has obtained more development and application in environmental protection.

Manganese titanate ($MnTiO_3$) has recently attracted much attention for its strong absorption in the visible region which may be propitious to the utilization of solar energy [7] and photocatalysis [8]. And also they are important due to their weak magnetism and semi conductivity [9, 10]. Zeolites are crystalline aluminosilicates containing pores and channels of molecular dimensions that are widely used in industry as ion exchange resins, molecular sieves, sorbents and catalysts [11-17].

In this study, $MnTiO_3$ nanoparticles and a series of $MnTiO_3$-Zeolite-Y nanocomposites were synthesized via stearic acid gel method. In addition characterization, magnetic and photo-catalytic properties of the nanocomposites were investigated.

2. Experimental

2.1. Materials

The chemicals used in this study are titanium (IV) n-butoxide as a titanium source and manganese acetate as manganese source-purchased from Aldrich chemical and stearic acid as a complexing reagent from Merck Co. purity of which is high. Also, Zeolite-Y was purchased from SPAG Co. Manganese titanate nanopowders were synthesized according to the previously reported method [18].

2.2. Preparation of $MnTiO_3$-ZY 5-10-20% nanocomposites

At first, $MnTiO_3$-ZY 5-10-20% nanocomposites are prepared by stearic acid gel method. Manganese acetate is added to the melted stearic acid and dissolved to form a dark red-brown transparent solution in this procedure. Then, titanium(IV) n-butoxide is slowly dropped into the mentioned solution. Further, stoichiometric amounts of Zeolite-Y are added to the mixed solution and stirred completely to obtain sol.

Cooling down is naturally the room temperature. Consequently, the gel is dried in oven at 100 °C for 12 h and calcined at 800-900-1000 °C for 4 h to obtain $MnTiO_3$-ZY nanocomposites.

3. Characterization:

To investigate the phase composition and crystalline size distribution of the nanocomposites after calcinations, x-ray powder diffraction (XRD) measurements are performed.XRD is recorded by Philips X-pert diffractometerabout10-90° for 2θ using Cu Kα radiation. The chemical identity of the products is afterward determined by comparing the experimental x-ray powder patterns to standard complied by the Joint Committee on powder diffraction and standards (JCPDS). The morphology of the product was studied by scanning electron microscopy (SEM, Philips XL30). Semiquantative analysis were carried out on an energy-dispersive x-ray spectrometer (EDAX) connected to XL30 Philips scanning electron microscope. The UV-Vis absorption spectra were obtained with 4802 Unico spectrophotometer in the region of 200-800 nm. To compare surface areas, total pore Volume and average pore diameter, BET analysis was studied by BelSorp Mini BEL Co. equipment. To investigate magnetic properties MDK6 equipment was used.

4. Results and discussion

4.1. XRD patterns

Fig. 1 shows the XRD patterns of 20% $MnTiO_3$-Zeolite-Y nanocomposites after heat treatment from 800 to 1000°C for 4 h in programmable temperature

furnace. Fig1a shows the characteristic peaks appeared at 2 θ =27.39°, 2θ=36.03°, 2θ = 33.22° that refer to TiO_2, Mn_2O_3 and Zeolite-Y respectively. Fig 1(b) shows the characteristic peak appeared at 2θ =21.96° that confirms the presence of rhombohedral $MnTiO_3$ phase in the nanocomposite. Further in Fig 1c by increasing the calcination temperature up to 1000°C a peak (2θ = 21.62°) was appeared that belongs to SiO_2 formation, instead of the nanocomposite.

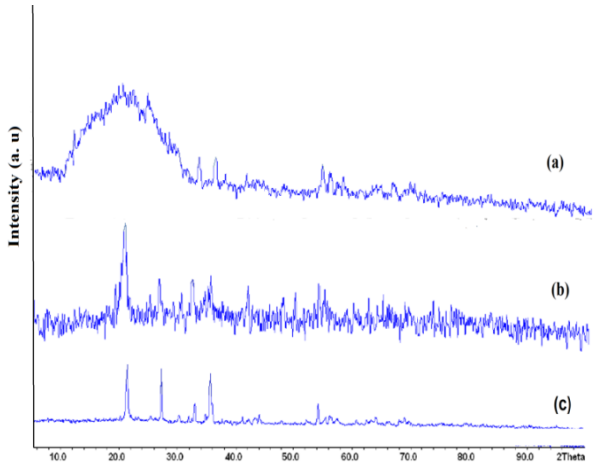

Fig. 1. XRD patterns of 20% $MnTiO_3$-Zeolite-Y nanocomposites calcined at 800 °C (a) 900 °C (b) 1000 °C (c).

Fig. 2 compares the 5-10-20% nanocomposites calcined at 900 °C for 4 h. The XRD patterns show that the intensity of $MnTiO_3$ peak in 20% nanocomposite is higher.

Table 1. Elemental analysis results of the 20% nanocomposite.

Element	At%	Wt%
AlK	15.43	11.45
SiK	49.00	37.84
TiK	15.52	20.44
MnK	20.05	30.28

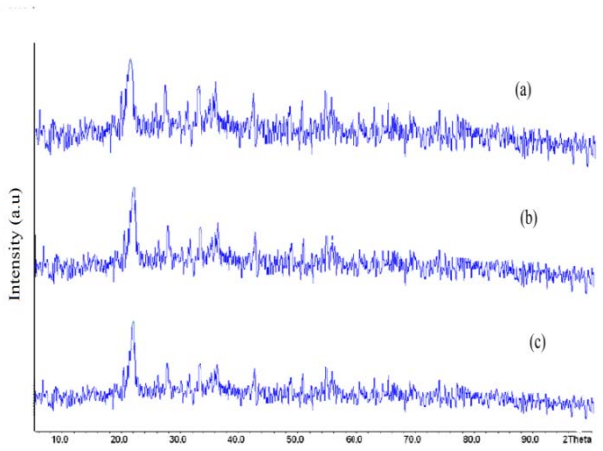

Fig. 2. XRD patterns of 5 %(a) -10 % (b) - 20% (c) $MnTiO_3$-Zeolite-Y nanocomposites calcined at 900°C

4.2. SEM and EDX studies

Fig. 3 (a-c) shows the typical SEM images of 5-10-20% nanocomposites respectively. The nano particle sizes are between 29-43 nm that agrees with the results of XRD. The stoichiometry of the obtained 20% nanocomposite was demonstrated by EDX measurement in Fig. 4. The elemental analysis results of 20% nanocomposite are showed in Table 1.

4.3. VSM result

Fig. 5 shows the vibration sample magnetism of 20% $MnTiO_3$-Zeolite-Y nanocomposite analysis. VSM result confirms that the magnetic property of 20% $MnTiO_3$-Zeolite-Y nanocomposite is antiferromagnetic.

4.4. BET comparison

This analysis is based on the BET theory which provides modeling of multi-layer adsorption of gas molecules. This method was used for identifying and

examining the pores on the surface of manganese titanate-zeolite-Y nanocomposite.

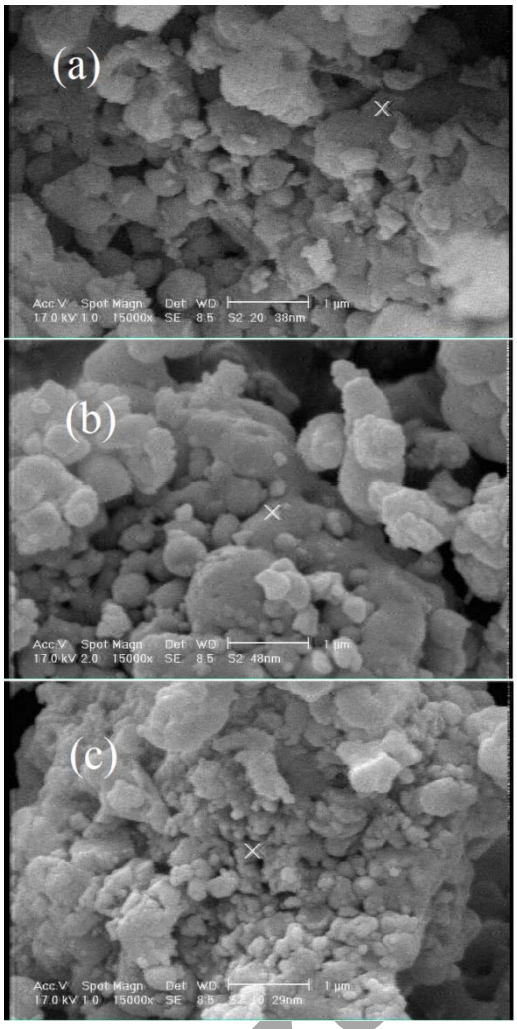

Fig. 3. SEM images of (a) 5% (b) 10% and (c) 20% $MnTiO_3$-Zeolite-Y nanocomposites.

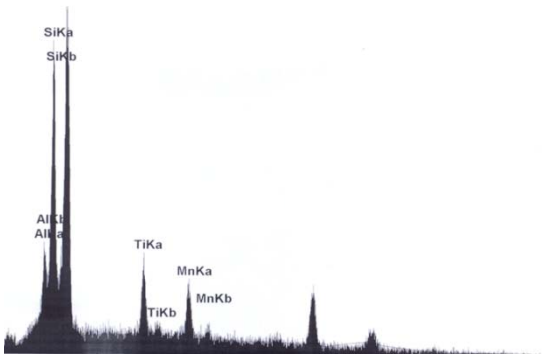

Fig. 4. EDX study of 20% $MnTiO_3$-Zeolite-Y nanocomposite.

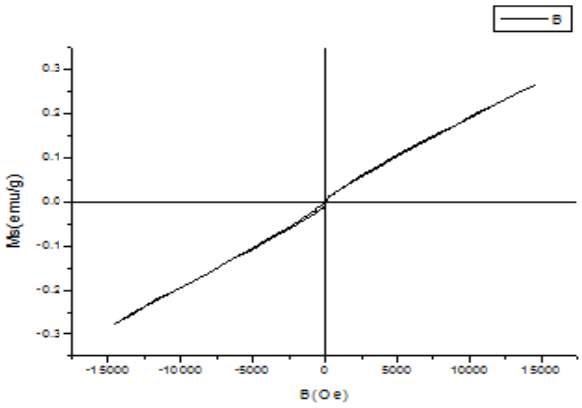

Fig. 5. VSM curve of 20% $MnTiO_3$-Zeolite-Y nanocomposites.

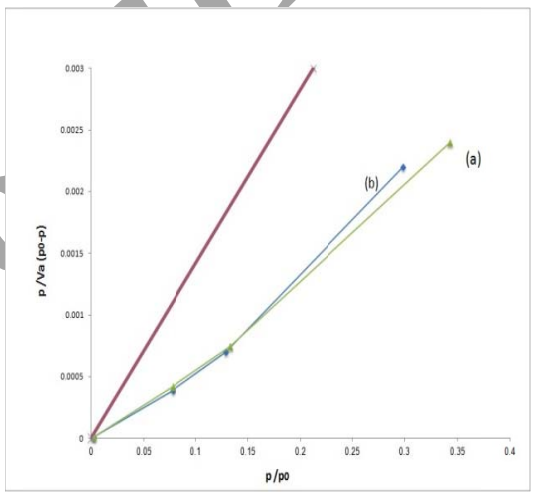

Fig. 6. BET comparison of zeolite-Y (a) and 20% $MnTiO_3$-Zeolite-Y nanocomposites (b).

Fig. 6 compares the BET analysis of Zeolite-Y and (20%) $MnTiO_3$-Zeolite-Y nanocomposite. The results are represented in table 2.

The difference between the specific surface and the average pore diameter of zeolite-Y and the nanocomposite shows that the growth of nanoparticles acts as a dam against the closure of the spaces in the structure of zeolite-Y. This is responsible for increment of the average diameter of pores. It also shows tha the-nano particles are distributed into the zeolite-Y. This combined with increment of average pore diameter and decrement

of specific surface of zeolite-Y. It is noteworthy that the small volume of pores can also confirms the presence of nanoparticles on the zeolite cavities.

Table 2. BET comparison results for nano composite and ZY.

Parameter	Nanocomposite	ZY	Unit
Vm	64.02	70.75	[cm^3g^{-1}]
as,BET	291.74	307.94	[m^2 g^{-1}]
C	10078.82	10079	cte
Total pore volume	0.362	0.4126	[cm^3 g^{-1}]
Average pore diameter	6.5421	5.3596	[nm]

4.5. UV-Vis spectra

Fig. 7. Shows the UV-Vis spectra that confirm the degradation of methylene blue solution (20 ppm) by 5-10-20% $MnTiO_3$-Zeolite-Y nanocomposites in the wavelength range of 200-800 nm. It proves that the 20% nanocomposite is more effective to decompose the structure of methylene blue molecules. It can be concluded from Fig.8 that 20% nanocomposite can decolorize the methylene blue solution (20ppm) up to 90% in 60 min.

Fig.9 shows the UV-Vis spectra that confirms the degradation of calcon solution (20 ppm) by 5-10-20% $MnTiO_3$-Zeolite-Y nanocomposites in the wavelength range of 200-800 nm.

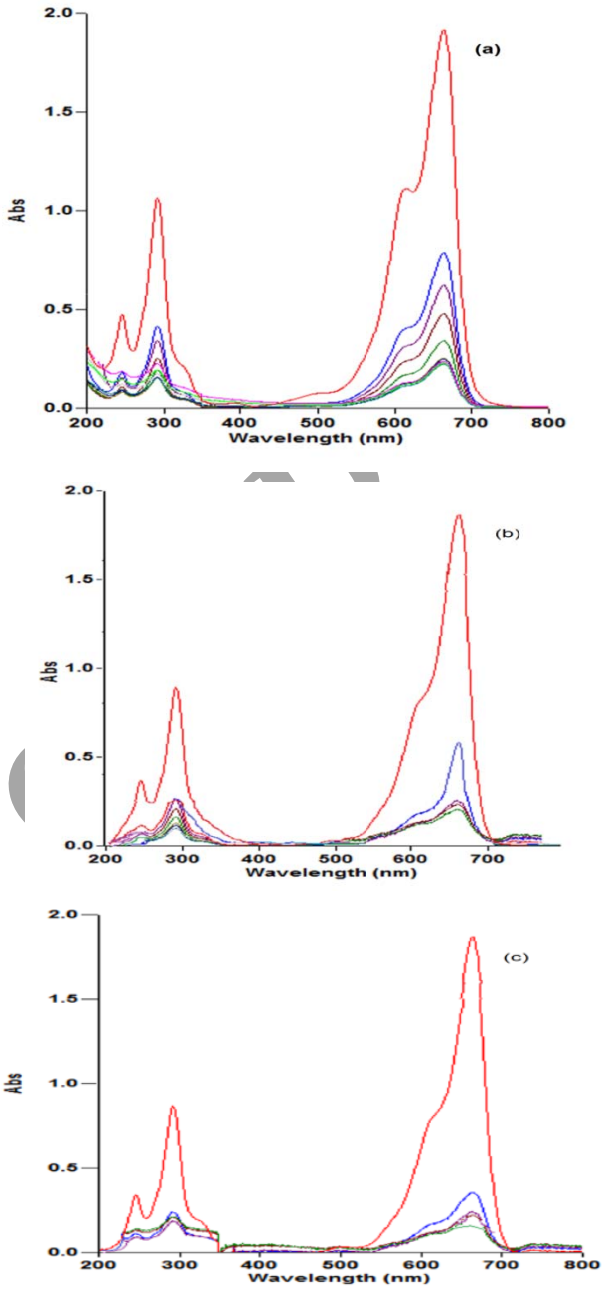

Fig. 7. UV-Vis spectra of 5 %(a)-10 % (b) 20% (c) $MnTiO_3$-Zeolite-Y nanocomposites.

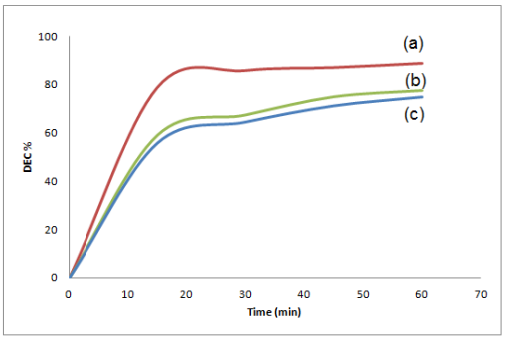

Fig. 8. Comparison of 5 % (a) -10 % (b) - 20% (c) $MnTiO_3$-Zeolite-Y nanocomposites for methylene blue decolorization.

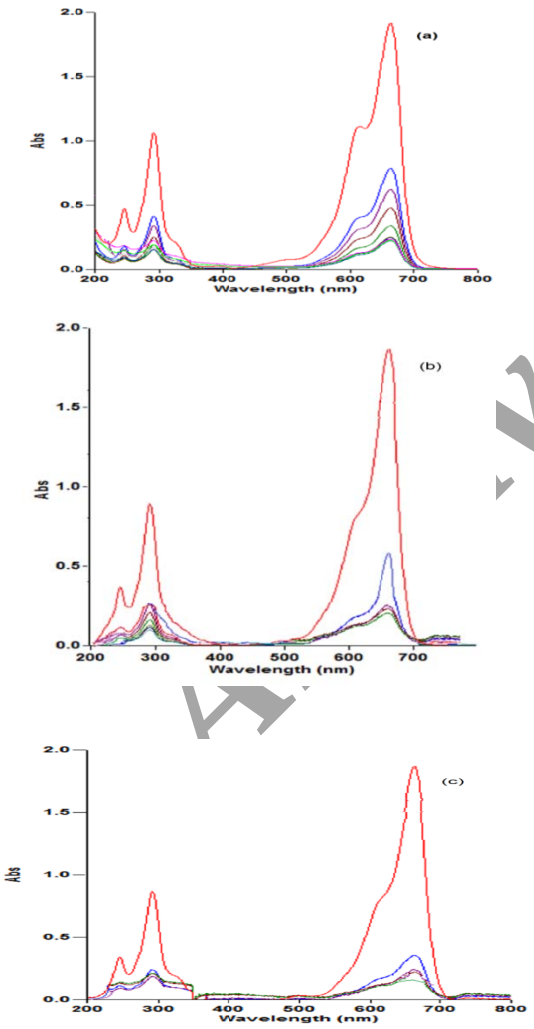

Fig. 9. UV-Vis spectra of 5 %(a) -10 % (b) - 20% (c) $MnTiO_3$-Zeolite-Y nanocomposites.

It proves that the 20% nanocomposite is more effective to decompose the structure of calcon molecules. It can be concluded from Fig. 10 that 20% nanocomposite can decolorize the calcon solution (20ppm) up to 63% in 60 min.

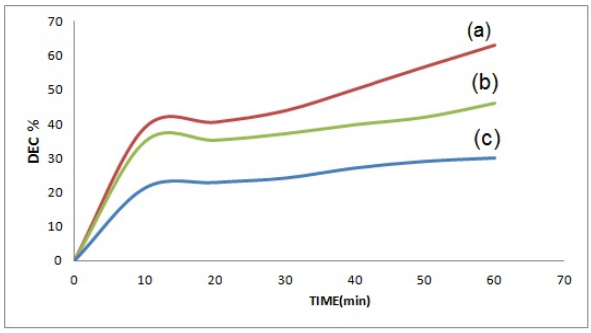

Fig. 10. Comparison of 5 %(a) -10 % (b) - 20% (c) $MnTiO_3$-Zeolite-Y nanocomposites for calcon decolorization.

5. Conclusion

$MnTiO_3$-ZYnanocomposites were synthesized with 5-10-20 %(w/w) by stearic acid gel method. The gel was calcined at 800, 900, 1000°Cfor 4 hours. The presence of rhombohedral phase of $MnTiO_3$ in Zeolite-Y matrix was confirmed by XRD. Scanning electron microscopy showed that the particle sizes are in the range of 29-43 nm. X-ray diffraction patterns and BET analysis showed the presence and growth of $MnTiO_3$ nanoparticles in Zeolite-Y. The VSM results showed the antiferromagnetic properties of 20% nanocomposite. The photocatalytic activity of the nanocomposites was evaluated by degradation of methylene blue and calcon reagents in aqueous solution. It can be concluded from UV-Vis spectra that the 20% nanocomposite can decolorize the methylene blue and calcon solutions (20 ppm) up to 90% and 63% respectively (both in 60 min). The best results were belonging to 20% nanocomposite.

Acknowledgements

Authors are grateful to the council of Islamic Azad University-North Tehran Branch and Iranian Nanotechnology Initiative for their unending effort to provide financial support to undertake this work.

References

[1] Y. Zhiyong, D. Laub, M. Bensimon, and J. Kiwi, Inorg. Chim. Acta., 361 (2008) 589–594.

[2] D.-E. Gu, B.-C. Yang, Y.D. Hu, Catal. Lett., 118 (2007) 254–259.

[3] C. Namasivayam, R. T. Yamuna, and J. Jayanthi, Cell. Chem. Technol., 37 (2003) 333–339.

[4] R. Dhodapkar, N. N. Rao, S. P. Pande, and S. N. Kaul, Bioresour. Technol. 97 (2006)877–885.

[5] B. Ohtani, Y. Ogawa, and S.-I.Nishimoto, J. Phys. Chem. B, 101(1997) 3746–3752.

[6] X. Chen, S. S. Mao, Chem. Rev., 107 (2007) 2891–2959.

[7] G.W. Zhou, Y.S. Kang, Mater. Sci. Eng. 24 (2004) 71-74.

[8] Z.Q.Song, S.B. Wang, W.Yang, M. Li, H. Wang, and H. Yan, Mater. Sci. Eng. B 113 (2004) 121-124.

[9] Zhou, G. W., Lee, D. K., Kim, Y.H., Kim, Y.H., Kim, Ch.W., Kang, Y.S., Korean Chem. Soc., 27(2006) 368-372.

[10] Arques, A., Amat, A. M., Juanes, L.S., Vercher, R.F., Marin, M. L., Miranda, M.A., J. Mol. Catal. A: Chem., 271 (2007) 221-226.

[11] X.Gu, J. Dong, T. M. Nenoff, Ind. Eng. Chem. Res. 44 (2005) 937–944.

[12] J. Hedlund, J. Sterte, M. Anthonis, A.-J.Bons, B.Carstensen, N. Corcoran, D. Cox, H. Deckman, W. D. Gijnst, P.-P. de Moor, F. Lai, J. McHenry, W. Mortier, J. Reinoso, J.Peters, Micropor. Mesopor. Mater. 52 (2002) 179-189.

[13] F. Bonhomme, M. E. Welk, T. M. Nenoff, Micropor, Mesopor, Mater 66 (2003) 181–188

[14] K. Kusakabe, T. Kuroda, A. Murata, S. Morooka, Ind. Eng. Chem. Res. 36 (1997) 649 – 655.

[15] M. P. Bernal, E. Piera, J. Coronas, M. Menendez, J. Santamaria, Catal. Today 56 (2000) 221-227.

[16] J. Sterte, S, Mintova, G. Zhang, B.J. Schoeman, Zeolites 18 (1997) 387–390.

[17] M. E. Davis, Nature 417 (2002) 813 –821.

[18] M. Enhessari, A. Parviz, E. Karamali, K. Ozaee, J. Exp. Nanosci. (2012) DOI:10.1080/17458080.2010.529173.